Welding in the World (2021) 65:1759–1765
https://doi.org/10.1007/s40194-021-01137-9

RESEARCH PAPER

Joining of the SiC$_f$/SiBCN composite with CoNiPdNbCr filler alloy and the control of the interfacial reactions

Wenwen Li[1] · Xinyu Ren[1] · Bo Chen[1] · Yongjuan Jing[1] · Huaping Xiong[1]

Received: 26 October 2020 / Accepted: 23 April 2021 / Published online: 17 May 2021

Abstract
The joining of the SiC$_f$/SiBCN composite was difficult due to the undue reactions between the SiC$_f$/SiBCN composite and the common Ni- or Co-based filler alloy. In this paper, a new filler alloy with the nominal composition of Co-20Ni-12Pd-18Nb-15Cr (wt.%) was newly designed to join the SiC$_f$/SiBCN composite. Compared with the BNi-5 filler alloy, the periodic banded structure in the reaction layer was eliminated. During the brazing process, the element Cr played an active role in the interfacial reactions and formed $Cr_{23}C_6$ layer at the surface of the SiC$_f$/SiBCN composite. The interfacial reaction layer could inhabit the diffusion of the elements Co and Ni to the SiC$_f$/SiBCN substrate. And then the interfacial reactions were controlled well. Under the brazing condition of 1200 °C/10 min, the average joint strength was increased from 18.2 to 54.9 MPa.

Keywords SiC$_f$/SiBCN composite · Interfacial reactions · Joint strength

1 Introduction

SiBCN ceramics have gained wide interest in recent years due to their excellent thermal stability, creep resistance, and oxidation resistance at high temperatures [1–4]. However, the monolithic SiBCN ceramic could not satisfy the requirements in the severe thermal shock environments because of the intrinsic brittleness. When continuous SiC fibers are embedded in the SiBCN matrix, the thermal shock resistance and fracture toughness of the ceramic composite were improved remarkably [5, 6], and thus, the SiC$_f$/SiBCN composite has been identified to be suitable for applications in the aerospace fields and anti-ablation structures, such as nose caps, satellite nozzles, and advance rocket engines [7, 8].

The practical use of the SiC$_f$/SiBCN composite requires development of appropriate joining techniques. Direct active brazing, due to its simplicity, lower cost investment, and potential as a mass production process, is the most common method for ceramic joining [9, 10]. Up to now, the joining technologies for SiBCN system materials also focused on brazing. Pan et al. [11] joined SiBCN and Nb using commercial AgCuTi filler assisted with Mo interlayer. Additionally, when joining SiBCN ceramic to TC4 alloy, TiB_2-reinforced AgTi composite filler was used for avoiding the formation of brittle Cu-Ti phase in the joint [12]. Another method to restrain reactions between the AgCuTi and TC4 was coating by SiC and TiB_2-reinforced TC4-based composite layers before the brazing process [13]. The composite layers could be treated as functionally graded material layers (FGM layers) and can effectively relieve the mismatch between SiBCN and TC4 alloy. Generally, AgCuTi system filler alloy can be widely applied to the joining of ceramics, and a reliable joint can be acquired with a service temperature lower than 500 °C [14–16]. However, AgCuTi filler alloy could not offer a high-quality SiBCN joint (joint shear strength was only 30~50 MPa at room temperature), even though assisted with Mo interlayer, TiB_2 reinforcement, and FGM layers. That is to say, the joining of SiBCN system materials is greatly different and more difficult compared with the Si_3N_4 and SiC ceramic.

Considering the fiber-reinforced SiBCN composites (CMCs), studies on the joining technology are extremely lacking. In our previous work, the joining of C$_f$/SiBCN composite was conducted with commercial BNi-5 filler alloy [17], Ni-Cr-Pd (Si,B) filler alloy [18] and CuPd-V [19] filler alloy. But these filler alloys cannot offer satisfactory joint strength. Compared with C$_f$/SiBCN, the high-temperature brazing of

---

Recommended for publication by Commission XVII - Brazing, Soldering and Diffusion Bonding

✉ Huaping Xiong
xionghp69@163.com; xionghuaping69@sina.cn

[1] Welding and Plastic Forming Division, Beijing Institute of Aeronautical Materials, Beijing 100095, China

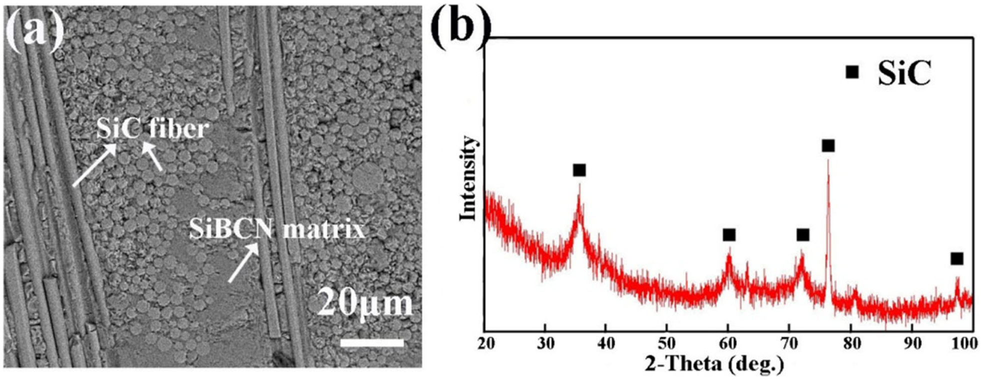

Fig. 1 The microstructure (**a**) and the XRD pattern (**b**) of the SiC_f/SiBCN composite

SiC_f/SiBCN composite has the obstacle that the intensive reactions of SiC with common elements Co and Ni resulted in the degradation of joint strength [20]. Up to now, there is no literature reporting about the SiC_f/SiBCN composite joining.

In this paper, a CoNiPdNbCr system filler alloy was newly designed for the joining of the SiC_f/SiBCN composite. The design of CoNiPdNbCr alloy was a result of the following considerations: firstly, elements Co and Ni are commonly used primary constituents in commercial superalloys. Correspondingly, the Co(Ni)-based brazing alloy matrix should have superior high-temperature properties [21]. Secondly, Pd has a large affinity with Si. As reported by references [22, 23], some Pd-containing filler alloys would react with SiC to form refractory Pd_2Si compound which can contribute to the high-temperature strength of the joint. Thirdly, it has been recognized that Cr and Nb are widely used in ceramic joining as active elements [18, 21]. At the same time, they are strong carbide-forming elements. The intensive reactions of filler alloy with silicon could be inhabited to some extent. Additionally, NbC was a refractory compound with a melting point of 3680 °C. The formation of NbC should be favorable for the joint high-temperature properties.

As a contrast, the commercial BNi-5 filler alloy (Ni-19Cr-10Si, wt.%) was also applied to the SiC_f/SiBCN joining. The interfacial reactions between the two filler alloys and SiC_f/SiBCN composite were analyzed respectively. The strengthening mechanism of the joint was also discussed.

2 Experimental procedures

SiC_f/SiBCN ceramic matrix composite was used as the base material to be joined, which was fabricated via resin transfer molding (RTM) and polymer infiltration and pyrolysis (PIP) [24]. The volume fraction of the SiC fibers was around 50%. The composition of amorphous matrix was $SiB_{0.17}C_{0.9}N_{1.04}O_{0.15}$. Figure 1 shows the microstructure of the base SiC_f/SiBCN composite and phase components measured by an X-ray diffraction (XRD) analyzer. It can be verified that, except for SiC phase, the SiC_f/SiBCN composite did not contain any additional crystalline phases from the systems Si-N or B-N.

The newly designed filler alloy has a nominal composition of Co-20Ni-12Pd-18Nb-15Cr (wt.%). The CoNiPdNbCr alloy ingot was fabricated by arc melting in an argon inert gas atmosphere. The ingot was molten at least 4 times to ensure the homogenous microstructure and chemical composition. A cylindrical specimen with a diameter of 3 mm and height of 3 mm was cut from the ingot for testing the melting point by differential scanning calorimetry (DSC). The DSC curve revealed a melting range from 1175 °C to 1205 °C, as shown in Fig. 2. The used filler foils were prepared by the rapidly solidified technology by a single-roller melt spinning equipment with a rotating Cu wheel [25], with the thickness of about 80~100 μm.

The composite samples to be joined were cut into 5 × 5 × 2 mm^3 plates for the metallographic observation and 2 × 4 × 20 mm^3 bars for four-point bend test, respectively. Additionally, three bars with a size of 2 × 4 × 40 mm^3 were also needed to evaluate the strength of the parent SiC_f/SiBCN composite. Before the assembly, all the specimens and the filler foils were cleaned with ethanol. The filler foil was placed between two SiC_f/SiBCN substrates or bars to form a butt joint. The fixed joints were heated to 1200 °C at a heating rate of 10 °C/min and kept at the brazing temperature for a dwelling time of 10 min. After brazing, the samples were cooled to 500 °C at a

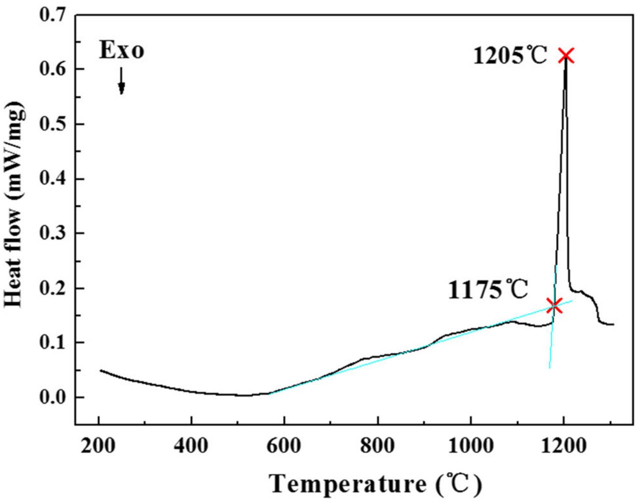

Fig. 2 DSC curve of the CoNiPdNbCr filler alloy

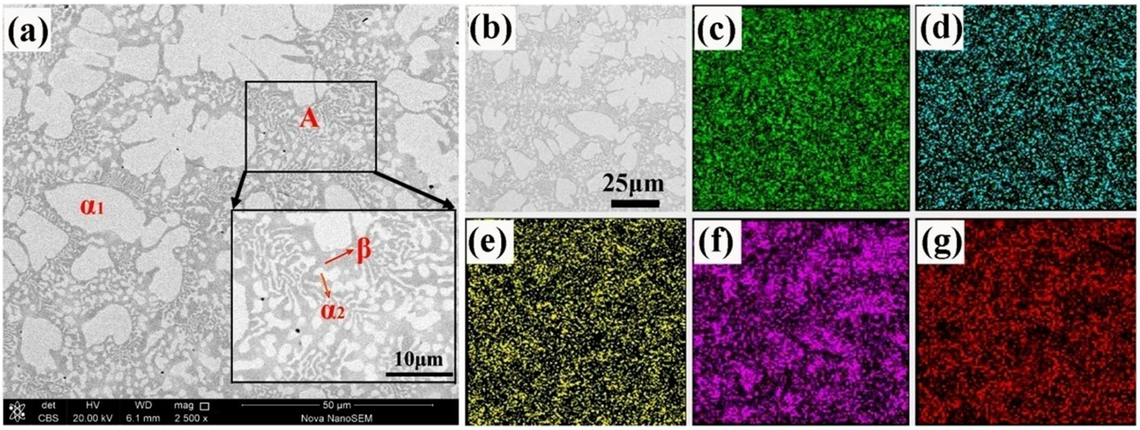

Fig. 3 Backscattered electron image and the magnification for the selected area A (**a**), and the elemental distribution maps for image (**b**): (**c**) Co, (**d**) Ni, (**e**) Pd, (**f**) Nb, and (**g**) Cr

cooling rate of 5 °C/min, followed by furnace cooling to room temperature. During the heating process, the vacuum of furnace was kept between 3.0 × 10^{-3}Pa and 7.0 ×10^{-3} Pa. The joint strength was measured by a four-point bend test at room temperature with a crosshead speed of 0.5 mm/min. Three specimens were tested for each experimental condition, and the joint strength is given in the form of error bars.

The microstructures of the ingot and the brazed joint were analyzed by a scanning electron microscope (SEM) equipped with an X-ray energy-dispersive spectrometer (EDS). For better phase identification, X-ray diffraction (XRD) analysis was performed on the filler alloy and an additional specimen of the SiC_f/SiBCN joint brazed at 1200 °C for 10 min. This specimen was prepared by a wetting experiment. Then, the unreacted brazing alloy at the outermost surface of the SiC_f/SiBCN substrate was moved away. Gradual polishing was conducted through the reaction zone at the sample surface, and XRD analysis was carried out successively on the surface containing the reaction layer.

3 Results and discussion

3.1 Microstructure of CoNiPdNbCr filler alloy

The microstructure of the as-casted CoNiPdNbCr alloy as well as the elemental distribution maps is shown in Fig. 3. It can be seen that the ingot microstructure was characterized by the primary α_1 phase and the eutectic (α_2+β) phase. According to the area distribution maps, elements Co, Ni, and Pd (Fig. 3c, d, and e) are distributed uniformly. But elements Nb and Cr exhibited segregation. Since element Nb has a higher atomic weight, the bright phase should be a niobium-rich phase.

Table 1 EDS analysis results for the typical microzones marked in Fig. 3a

Microzone	Composition (at %)					Deduced phase
	Co	Ni	Pd	Nb	Cr	
α_1	43.99	15.13	5.64	21.78	13.45	(Co,Ni)$_3$Nb dissolved with (Pd,Cr)
α_2	41.89	17.86	8.13	18.31	13.81	
β	39.34	19.99	9.82	4.14	26.7	Co(Cr,Ni)ss

The EDS analysis results for these phases are listed in Table 1, signifying that the constitution of the primary phase α_1 was nearly identical to that of α_2 in eutectic structure. So both the α_1 phase and α_2 phase can be simply defined as α phase. The concentration of niobium in α phase was much higher than in β phase. On the contrary, the Cr element has a higher concentration in β phase. However, for the elements Co, Ni, and Pd, there was no difference in concentration between phases α and β.

X-ray diffraction analysis was performed in order to verify the phases identified by SEM and EDS, as shown in Fig. 4. The XRD peaks have good correspondence to the Co_3Nb phase, Ni_3Nb phase, and Co-based solid solution.

In the CoNiPdNbCr system alloy, the mixing enthalpy of Co/Nb and Ni/Nb is very negative (− 25 kJ/mol and − 30 kJ/mol, respectively [26]); it was inclined to form the

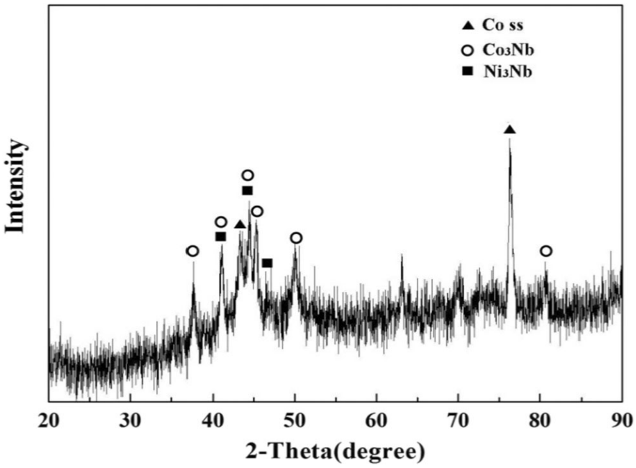

Fig. 4 XRD pattern of the as-casted CoNiPdNbCr filler alloy

Fig. 5 Microstructure of the SiC_f/SiBCN composite joint brazed with BNi-5 filler alloy

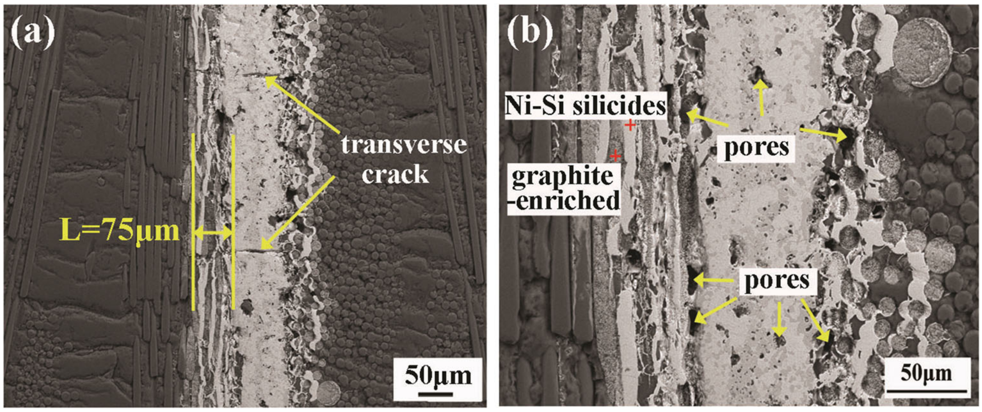

intermetallics. In the meantime, the mixing enthalpy of Co/Ni, Co/Pd, and Co/Cr was 0 kJ/mol, − 1 kJ/mol, and − 4 kJ/mol, respectively. As a result, the solid solution was easily formed among the elements Co, Ni, Pd, and Cr.

3.2 Joining of the SiC_f/SiBCN composite

Figure 5 shows the microstructure of the SiC_f/SiBCN joint brazed with BNi-5 filler alloy. It can be seen that interfacial reactions between the BNi-5 filler alloy and the SiC_f/SiBCN composite were very intensive. The reaction distance was 75 μm as pointed in Fig. 5a. Meanwhile, some transverse cracks formed across the brazing seam. As shown in Fig. 5b, the over-reactions resulted in a periodic banded structure which consisted of alternating Ni-silicide bands and graphite-enriched band. The joint exhibited a low four-point bend strength of 18.2 MPa at room temperature. This phenomenon is common when joining the SiC ceramic with Co- or Ni-based filler alloys, and the periodic banded structure weakened the mechanical properties of the joints [27].

When brazed with the newly designed filler alloy, the joint microstructure has been changed completely, and the periodic banded structure was eliminated, as shown in Fig. 6a. Meanwhile, the corresponding elemental distribution maps are also presented in Fig. 6.

From the distribution maps (Fig. 6f), it can be seen that element Cr enriched at the SiC_f/SiBCN composite interface obviously. So that Cr played an active role in the interfacial reactions during the brazing process. The EDS analysis results (listed in Table 2) also proved that the elements Cr and C were enriched in microzones “1” and “2.” It is known that different types of chromium carbides exist, namely $Cr_{23}C_6$, Cr_7C_3, and Cr_3C_2. Using thermodynamic data, the Gibbs free energy of formation of selected metal carbides can be calculated; for example, at 1200 °C, that of $Cr_{23}C_6$, Cr_7C_3, and Cr_3C_2 is − 398 kJ/mol, − 196 kJ/mol, and −100 kJ/mol, respectively [28]. Therefore, from the thermodynamic point of view, the most likely carbide to form in this system should be $Cr_{23}C_6$. The XRD pattern for the interface between the SiC_f/SiBCN and CoNiPdNbCr filler alloy is shown in Fig. 7, in which the $Cr_{23}C_6$ compound was indeed detected.

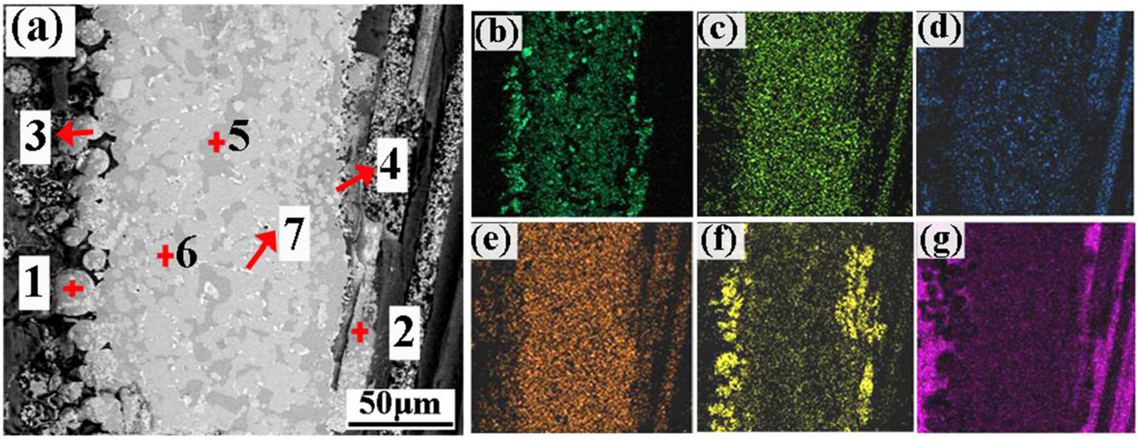

Fig. 6 Microstructure of the SiC_f/SiBCN composite joint brazed with CoNiPdNbCr filler alloy (**a**), and area distribution maps of elements Nb (**b**), Ni (**c**), Pd (**d**), Co (**e**), Cr (**f**), and Si (**g**)

Table 2 EDS analysis results for the typical microzones in Fig. 6a

Microzone	Composition (at. %)									Deduced phase
	Co	Ni	Pd	Nb	Cr	Si	B	C	N	
1	1.25	/	0.16	/	43.5	1.48	/	53.6	/	$Cr_{23}C_6$
2	7.04	1.83	0.2	2.41	24.54	6.84	/	57.14	/	$Cr_{23}C_6$
3	1.91	1.14	3.91	25.49	0.89	2.81	/	63.85	/	NbC
4	0.58	0.35	/	29.85	0.57	0.24	/	68.42	/	NbC
5	35.6	16.34	4.03	/	10.8	33.24	/	/	/	$(Co,Ni)_2Si$
6	21.92	10.0	0.81	11.71	1.5	14.11	/	39.96	/	$(Co,Ni)_2Si$/NbC
7	6.88	7.58	52.29	/	1.45	31.8	/	/	/	Pd_2Si

Considering the element Nb, it also exhibited interfacial reaction activity to some extent from the distribution map in Fig. 6b. Near the SiC_f/SiBCN interface, the light gray phases in microzones "3" and "4" were enriched with niobium and carbon. Combined with the XRD results, NbC compounds should be formed here. For microzone "5," 35.6% Co, 16.34% Ni, and 33.24% Si were detected here. It can be deduced that $(Co,Ni)_2Si$ silicides have formed. The XRD analysis of the prepared reaction layer of the wetting specimen confirmed the formation of Co_2Si and Ni_2Si. There is a lot of gray phase labeled by "6", with the composition of 21.92 % Co, 10.0% Ni, 11.71% Nb, 14.11% Si, and 39.96 % C, indicating the predominant reaction products of $(Co,Ni)_2Si$. Meanwhile, the appearance of Nb proved that the element Nb not only enriched at the interface but also distributed in the central part of the joint. This can be confirmed by the distribution map of Nb shown in Fig. 6b. According to the EDS analysis, the NbC compound was formed together with the $(Co,Ni)_2Si$ in microzone "6".

Noticeably, some tiny white phase "7" is scatteringly distributed in the central part of the joint. The atomic ration of Pd and Si was near 2:1 according to the EDS analysis. It should be the Pd_2Si refractory compound. However, there was no Pd_2Si phase detected by XRD. It has been demonstrated that element Pd has a large affinity with Si [29]. The formation of Pd_2Si compounds was a common phenomenon when joining Si_3N_4 [30] and C_f/SiC composites [31] using Pd-containing filler alloys. Therefore, the formation of Pd_2Si compounds through the reaction between the SiC_f/SiBCN composite and the CoNiPdNbCr filler alloy is not unexpected.

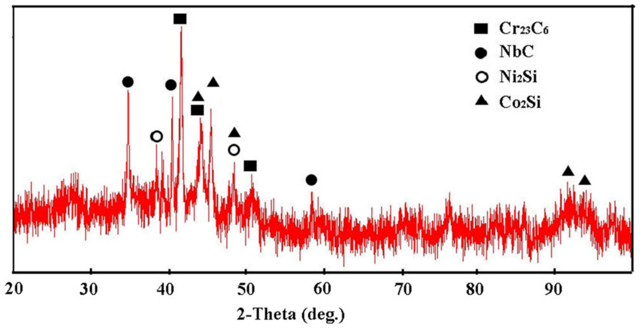

Fig. 7 XRD pattern of the prepared reaction layer of the wetting specimen

The overall reactions between the SiC_f/SiBCN composite and the filler alloy during the brazing procedure can be concluded as follows:

$$Cr + C \rightarrow Cr_{23}C_6 \quad (1)$$

$$Nb + C \rightarrow NbC \quad (2)$$

$$Co + Ni + Si \rightarrow (Co, Ni)_2Si \quad (3)$$

$$Pd + Si \rightarrow Pd_2Si \quad (4)$$

When using the BNi-5 filler alloy, element Ni diffused into the SiC_f/SiBCN composite and reacted intensively. Meanwhile, Si atoms diffused into the liquid filler alloy. So the joint microstructure can be characterized by the Ni-Si/graphite periodic banded structure at the interface and the brittle silicides in the brazing seam, as shown in Fig. 8.

However, when brazed with the newly designed CoNiPdNbCr filler alloy, elements Cr and Nb played an active role in the interfacial reactions. The formation of $Cr_{23}C_6$ reaction layer at the interface showed an effect on inhabiting the reaction between Co, Ni and the SiC_f/SiBCN composite. The interfacial reaction was thus depressed remarkably. Xiong et al. studied the control of the interfacial reactions between SiC ceramic and Co-based filler alloy [32], and it was found that active elements V and Ti added into the filler alloy can eliminate the periodic structure.

The joints brazed with the two filler alloys were tested for their four-point bend strength at room temperature, as shown in Fig. 9. It can be seen that the strength of the joint brazed with the CoNiPdNbCr filler alloy was

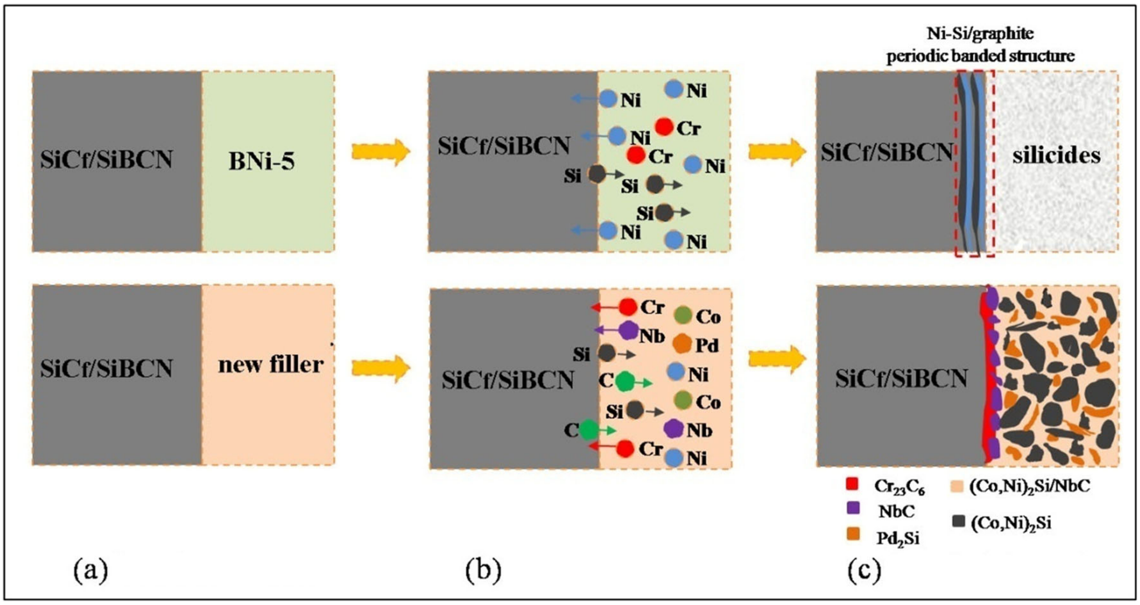

Fig. 8 Comparison of the interfacial reaction mechanism

improved significantly from 18.2 to 54.9 MPa. Under the same condition, the average four-point bend strength of the base SiC_f/SiBCN composite was 161.5MPa. That is to say, the strength of the brazed SiC_f/SiBCN joint has reached up to 34% of that of the base material. On one hand, the interfacial reactions were depressed and the periodic banded structure was eliminated, so that the bonding strength can be improved. On the other hand, the joint microstructure was composed of $(Co,Ni)_2Si$, NbC, and Pd_2Si compounds, rather than the monolithic silicides in the case of BNi-5. To some extent, the joint brittleness was decreased and thus the joint strength could be improved. However, deeper studies are still needed in future concerning the new filler alloys with better performance not only for ceramic composite joining but also for its component repair [33–35].

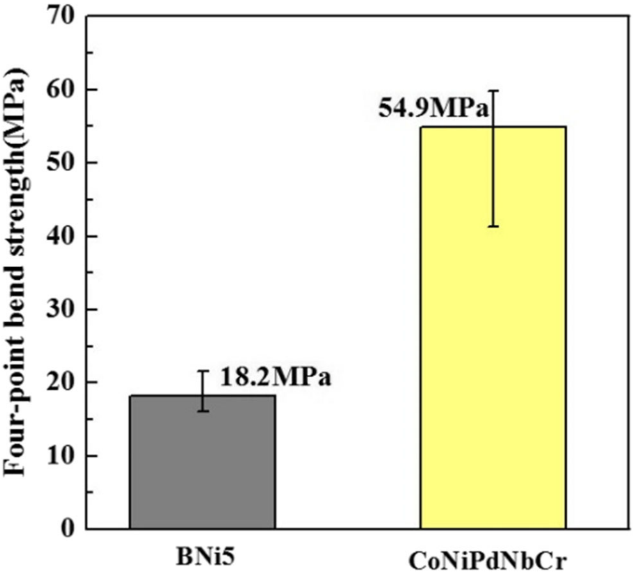

Fig. 9 Four-point bend strength of the SiC_f/SiBCN joints tested at room temperature

4 Conclusions

In order to control the interfacial reactions, a CoNiPdNbCr filler alloy was newly designed to join the SiC_f/SiBCN composite. When brazed with BNi-5 filler alloy, the joint microstructure consisted of the Ni-Si/graphite periodic banded structure at the interface and the brittle silicides in the brazing seam, and the joint strength was only 18.2 MPa.

When using CoNiPdNbCr filler alloy to join the SiC_f/SiBCN composite at 1200 °C for 10 min, element Cr played an active role in the interfacial reactions and formed $Cr_{23}C_6$ reaction layer at the SiC_f/SiBCN composite. In the central part of the joint, the matrix was formed of $(Co,Ni)_2Si$ and NbC compounds. Meanwhile, the Pd_2Si and $(Co,Ni)_2Si$ phases were scatteringly distributed. The $Cr_{23}C_6$ reaction layer inhabited the mutual diffusion between SiC_f/SiBCN and the filler metal. The interfacial reactions were depressed significantly and the periodic banded structure was eliminated. The joint was strengthened and the joint strength was improved to 54.9 MPa.

Funding This work was sponsored by the National Nature Science Foundation of China under grant nos. 59905022, 50475160, 51775525 and 51275497, and Aeronautical Science Foundation of China under grant 2008 ZE21005.

References

1. Riedel R, Kienzle A, Dressler W, Ruwish L, Bill J, Aldinger F (1996) A siliconboron carbonitride ceramic stable to 2000°C. Nature 382:796–798
2. Zhang PF, Jia DC, Yang ZH, Duan XM, Zhou Y (2012) Progress of a novel non-oxide Si-B-C-N ceramic and its matrix composites. J Adv Ceram 1:157–178
3. Weinmann M, Schuhmacher J, Kummer H, Prinz S, Peng JQ, Seifert HJ, Christ M, Müller K, Bill J, Aldinger F (2000) Synthesis and thermal behavior of novel Si-B-C-N ceramic precursors. Chem Mater 12:623–632
4. Kumar R, Phillipp F, Aldinger F (2007) Oxidation induced effects on the creep properties of nano-crystalline porous Si-B-C-N ceramics. Mater Sci Eng A 445-446:251–258
5. Liang B, Yang ZH, Li YT, Yuan JK, Jia DC, Zhou Y (2015) Ablation behavior and mechanism of SiC$_f$/C$_f$/SiBCN ceramic composites with improved thermal shock resistance under oxyacetylene combustion flow. Ceram Int 41:8868–8877
6. Sun M, Fu R, Chen J, Mao X, Zhang J, Yang Z, Liang B (2016) Fabrication and microstructures of functional gradient SiBCN-Nb composite by hot pressing. Mater Charact 114:115–121
7. Baldus P, Jansen M, Sporn D (1999) Ceramic fibers for matrix composites in high-temperature engine applications. Science 285: 699–703
8. Wang JY, Duan XM, Yang ZH, Jia DC, Zhou Y (2014) Ablation mechanism and properties of SiC$_f$/SiBCN ceramic composites under an oxyacetylene torch environment. Corros Sci 82:101–107
9. Beura VK, Xavier V, Venkateswaran T, Kulkarni KN (2018) Interdiffusion and microstructure evolution during brazing of austenitic martensitic stainless steel and aluminum-bronze with Ag-Cu-Zn based brazing filler material. J Alloys Compd 740:852–862
10. Liu D, Niu HW, Zhou YH, Song XG, Tang DY, Feng JC (2015) Brazing continuous carbon fiber reinforced Li$_2$O-Al$_2$O$_3$-SiO$_2$ ceramic matrix composites to Ti-6Al-4V alloy using Ag-Cu-Ti active filler metal. Mater Des 87:42–48
11. Pan R, Kovacevic S, Lin T, He P, Sekulic DP, Mesarovic SD, Yang Z, Shen Y, Wei H (2016) Control of residual stresses in 2Si-B-3C-N and Nb joints by the Ag-Cu-Ti+Mo composite interlayer. Mater Des 99:193–200
12. Shi JM, Zhang LX, Liu H, Sun Z, Feng JC (2018) Vacuum brazing of SiBCN ceramic and TC4 alloy using TiB$_2$ reinforced AgTi composite filler. Vacuum 156:108–114
13. Shi JM, Zhang LX, Liu H, Sun Z, Feng JC (2019) Reliable brazing of SiBCN ceramic and TC4 alloy using AgCuTi filler with the assist of laser melting deposited FGM layers. J Mater Sci 54: 2766–2778
14. Peteves SD, Nicholas MG (1996) Evaluation of brazed silicon nitride joints: microstructure and mechanical properties. J Am Ceram Soc 79(6):1553–1562
15. Liu Y, Huang ZR, Liu XJ (2010) SiC reaction layer microstructure of SiC/SiC joints brazed by Ag-Cu-Ti filler metal. Key Eng Mater 434-435:202–204
16. Chen B, Zou W, Li W, Wu S, Xiong H (2017) Joining of SiO$_{2f}$/SiO$_2$ composite to Ti-6Al-4V using Ag-Cu-In-Ti brazing fillers, the joint strengths and microstructures. Weld World 61:833–837
17. Li W, Chen B, Xiong Y, Xiong H, Cheng Y, Zou W (2017) Joining of C$_f$/SiBCN composite with two Ni-based brazing fillers and interfacial reactions. J Mater Sci Technol 33:487–491
18. Li W, Chen B, Xiong H, Cheng Y, Wu X, Ren H (2019) Joining of C$_f$/SiBCN composite with a Ni-Cr-Pd(Si,B) filler alloy. J Mater Eng Perform 28:6746–6752
19. Li W, Chen B, Cao L, Liu W, Xiong H, Cheng Y (2018) Joining of C$_f$/SiBCN composite with CuPd-V filler alloy. J Mater Sci Technol 34:1652–1659
20. Xiong HP, Mao W, Xie YH, Chen B, Guo WL, Li XH, Cheng YY (2007) Control of interfacial reactions and strength of the SiC/SiC joints brazed with newly-developed Co-based brazing alloy. J Mater Res 22:2727–2736
21. Li W, Chen B, Xiong H, Zou W (2017) Brazing SiC matrix composites using Co-Ni-Nb-V alloy. Weld World 61:839–846
22. Xiong HP, Chen B, Pan Y, Mao W, Cheng YY (2014) Interfacial reactions and joining characteristics of a Cu-Pd-V system filler alloy with C$_f$/SiC composite. Ceram Int 40:7857–7863
23. Xiong HP, Chen B, Zhao HS, Cheng YY (2016) V-containing active high-temperature brazes for ceramic joining. Weld World 60:99–108
24. Tan X, Liu W, Cao L, Dai S (2018) Oxidation behavior of a 2D-SiC$_f$/BN/SiBCN composite at 1350-1650°C in air. Mater Corros 69:1227–1236
25. Li XQ, Li L, Hu K, Qu SG (2015) Vacuum brazing of TiAl-based intermetallics with Ti-Zr-Cu-Ni-Co amorphous alloy as filler metal. Intermetallics 57:7–16
26. Takeuchi A, Inoue A (2005) Classification of bulk metallic glasses by atomic size difference, heat of mixing and period of constituent elements and its application to characterization of the main alloying element. Mater Trans 12:2817–2829
27. Chou TC (1993) Interfacial debonding by solid-state reactions of SiC with Ni and Co. Scr Met Mater 29:255–260
28. Park JS, Landry K, Perepezko JH (1999) Kinetic control of silicon carbide/metal reactions. Mater Sci Eng A 259:279–286
29. Bhanumurthy K, Schuster JC (2001) Interface reactions between silicon carbide and metals (Ni,Cr,Pd,Zr). Compos Part A 32:569–574
30. Sun Y, Zhang J, Geng YP, Ikeuchi K, Shibayanagi T (2011) Microstructure and mechanical properties of an Si$_3$N$_4$/Si$_3$N$_4$ joint brazed with Au-Ni-Pd-V filler alloy. Scr Mater 64:414–417
31. Xiong HP, Chen B, Pan Y, Ye L (2014) Joining of C$_f$/SiC composite with a Cu-Au-Pd-V brazing filler and interfacial reactions. J Eur Ceram Soc 34:1481–1486
32. Xiong H, Chen B, Kang Y, Mao W, Kawasaki A, Okamura H, Watanabe R (2007) Wettability of Co-V, and PdNi-Cr-V system alloys on SiC ceramic and interfacial reactions. Scr Mater 56:173–176
33. Lusquiños F, Pou J, Quintero F, Pérez-Amor M (2008) Laser cladding of SiC/Si composite coating on Si–SiC ceramic substrates. Surf Coat Technol 202(9):1588–1593
34. Chen B, Zou W, Li W, Wu S, Xiong H, Wu X (2020) Joining of SiO$_{2f}$/SiO$_2$ composite to Nb using Ag-Cu-In-Ti brazing alloys. J Mater Sci Technol 50:13–20
35. Li N, Huang S, Zhang G, Qin R,Liu W, Xiong H, Shi G, Blackburn J (2019) Progress in additive manufacturing on new materials: A review. J Mater Sci Technol 35(2):242–269